J. Physiol. (1981), **310**, *pp.* 159–190
With 8 text-figures
Printed in Great Britain

THE KINETICS OF SLOW MUSCLE ACETYLCHOLINE-OPERATED CHANNELS IN THE GARTER SNAKE

BY VINCENT E. DIONNE

From the Division of Pharmacology, Department of Medicine, University of California at San Diego, La Jolla, California 92093, U.S.A.

(*Received 6 December 1979*)

SUMMARY

1. Slow muscle synaptic responses were modelled kinetically in an attempt to define the mechanism by which slow fibre acetylcholine-operated channels differ from those in twitch fibres.

2. Three kinetically distinguishable states were necessary.

3. All applicable three-state kinetic schemes were considered in an attempt to identify the simplest description of the data. Experimental tests eliminated several models. Two models were not tested because they contained an excessive number of adjustable parameters.

4. The data were not fitted by kinetic schemes which postulated (i) channels which opened with one as well as two bound agonist molecules, (ii) channels which became blocked after opening, or (iii) separate populations of synaptic and extrasynaptic channels.

5. The three-state kinetic model of del Castillo & Katz (1957) accurately described all the data. This sequential model relates a closed channel state with no agonist bound to its receptors, an intermediate state (also closed) with agonist bound, and an open channel state. It is the same model which has been used to describe synaptic responses in twitch fibres.

6. The variation which allows this model to describe both twitch and slow fibre synaptic responses is the lifetime of the intermediate state. In twitch fibres the intermediate state lifetime is undetectably brief by electrophysiological methods. However, in slow fibres this lifetime appears to be 1–2 msec, varying with voltage.

7. Three of the four transition rates in this three-state kinetic scheme may be estimated by fitting the model to the data. These are the channel opening rate, the channel closing rate and the rate at which closed channels lose their bound agonist molecules. The latter two rates appear to depend exponentially on voltage. The channel opening rate was not detectably voltage-sensitive.

INTRODUCTION

The value of kinetic analysis as a means of elucidating the mechanisms of membrane conductance changes is now widely appreciated. Applications of this analytical technique to synaptic channels began after Katz & Miledi (1970) showed that the

0022-3751/81/2950-0652 $07.50

end-plate voltage noise which developed in muscle cells with the exogenous application of acetylcholine (ACh) was produced by the inherent properties of a membrane mechanism and was not incidental to it. Following that report, Anderson & Stevens (1973) employed the voltage clamp to demonstrate that end-plate voltage fluctuations arose from fluctuations in membrane conductance due to moment-to-moment variations in the number of open ACh-operated channels. Kinetic analysis of the conductance fluctuations allowed them to estimate the mean conductance of a single channel, mean open channel lifetime, and in addition to make quite plausible suggestions of the source of channel lifetime voltage dependence. Subsequent work (cf. Neher & Stevens, 1977; Cull-Candy, Miledi & Trautwein, 1979; Anderson, Cull-Candy & Miledi, 1978; Barker & McBurney, 1979) has demonstrated the wide applicability and usefulness of the method. In the process the quantitative methods of kinetic analysis as applied to membrane conductance systems has been treated by several authors, most generally by Colquhoun & Hawkes (1977).

In this paper I present a kinetic analysis of synaptic responses from snake slow (tonic) muscle neuromuscular junctions. As described in a previous paper (Dionne & Parsons, 1980), slow fibre synaptic responses differ from those in twitch fibres, being more complex in the sense that they cannot be fitted by the predictions of a two-state kinetic scheme. Miniature end-plate currents (impulse response), end-plate current relaxations following a sudden voltage change (step response) and end-plate current fluctuations (equilibrium response), all produced by the natural transmitter acetylcholine, were studied because they provide quite different but complementary information. The miniature end-plate currents decayed as a single exponential component, while both the step response and the fluctuations gave persistent evidence of at least two components.

These two-component responses could be modeled by linear kinetic schemes of three or more states; for simplicity only models with three kinetically distinguishable states were considered. There are six models which might be applied. While it would have been preferable to select among these six models on experimental criteria alone, that was not possible. Nevertheless, experimental measurements have shown that the slow fibre responses do not arise because they are mediated by some channels opening with one and others with two molecules of acetylcholine, by the blocking of open channels or by extrasynaptic receptors. The results are consistent with a channel which can open and close several times once its receptors have bound the necessary agonist molecules.

METHODS

These experiments were performed on slow muscle fibres in garter snake (sp. *Thamnophis*) costocutaneous muscles. The experimental methods were those described by Dionne & Parsons (1980). In addition, the voltage-step experiments were performed under conditions of ACh concentration and distribution identical to those for the recording of end-plate current fluctuations. To achieve this, the same ACh ionophoretic electrode position, current amplitude and time course were used to induce the membrane conductance change during each response type. The cells were held at a nominal resting voltage, hyperpolarized about 40 mV by a command pulse to a prestep potential, then returned to the resting voltage; the step response data were collected following the depolarizing return step. The pulse duration at the prestep potential was 250 msec, sufficiently long for equilibrium conditions to be established before depolarizing to the test (resting) voltage. This protocol allowed miniature end-plate currents (m.e.p.c.s) and noise

as well as the step response to be recorded at the same voltage while avoiding conditions which cause the resting membrane conductance to change.

Experimental tests of the kinetic theories required sets of measurements at different membrane voltages or at fixed voltage with different mean end-plate currents (e.p.c.). Both protocols required the slow muscle cell to remain stable for a prolonged period, but many cells were incapable of this. They deteriorated rapidly, typically becoming unusable within about 20 min. Thus, some of the conclusions drawn here rest to an extent on data acquired in those rare cells which tolerated the recording conditions well. Nevertheless, of the cells studied (more than 100), all gave results which were consistent with the description which follows.

Three measurable parameters were estimated by fitting theory to data; these were two apparent decay rates associated with two separate response components and the relative amplitude of the two components. The technique used to fit the data allowed a moderate degree of flexibility in evaluating these measurable parameters. However, because one of the two rates could be accurately obtained from the m.e.p.c. decay, the uncertainty of the estimates was not as severe as would have been the case with all parameters free (Neher & Stevens, 1977). First the decay rate of the m.e.p.c. was determined. The companion noise spectrum was then fit with the sum of two Lorentzian (1/frequency^2) components; one corner frequency was constrained by the m.e.p.c. rate while the relative amplitude of the components and the second corner frequency were adjustable. These two adjustable parameters were varied to obtain the best visual fit (e.g. Fig. 1*B*). The equivalence of the observed rates in the equilibrium, step and impulse responses is a general result of the kinetic analysis and will become apparent in the theoretical section which follows. In a set of later experiments where voltage-step responses were also obtained, the rates determined from the m.e.p.c.s and spectra were used to predict the time course of the step response.

From several cells m.e.p.c. and noise data were obtained at three or more voltages; these data were used to derive estimates of the transition rates and state lifetimes with the KM model (scheme 13). In all cases the derived rate β showed considerable variation but little reliable evidence of voltage sensitivity. Similarly, other laboratories have reported little or no voltage sensitivity for the apparent activation rate of the cholinergic channel (Gage & McBurney, 1975; Neher & Sakmann, 1975; Sheridan & Lester, 1975; Dionne & Stevens, 1975; Adams, 1976). With this data the two adjustable parameters were altered slightly so as to limit the variability of estimated β with voltage in individual cells. Variation of the fitting parameters was constrained by the requirement that the quality of the spectral fit be as high as possible. This procedure not only limited the range of the derived β values but also markedly improved an already clear logarithmic dependence of the derived quantities τ_1, τ_2, α and k_2 on voltage (KM model). Such an optimization of the fitting procedure was not carried out systematically to any final minimum variance for β or any other quantity. Finally, no variation of this sort caused the discounted kinetic theories to fit the data more accurately.

RESULTS

Experimental observations

Of the three synaptic responses elicited from slow muscle fibres utilized here, two were described in a previous paper (Dionne & Parsons, 1981) which dealt with response characteristics. The basic features were (1) in the majority of fibres the slow fibre m.e.p.c. decayed as a *single* exponential with time (Fig. 1*A*), and (2) the ACh noise spectrum was *not* a single Lorentzian component (Fig. 1*B*). If a two-state kinetic scheme were to describe these synaptic responses one would expect an exponential m.e.p.c. and a Lorentzian spectrum related by their decay time constant τ and corner frequency f_0 as $\tau = 1/2\pi f_0$. Although the major time constant in the slow fibre spectrum was indeed a Lorentzian component so related to the m.e.p.c. (Dionne & Parsons, 1978), additional high frequency noise power appeared in about 60% of the cells which could never be predicted by a two-state kinetic scheme. Thus,

while a two-state kinetic model was completely satisfactory for garter snake twitch fibre responses (Dionne & Parsons, 1981) as well as those in frog (Anderson & Stevens, 1973; Neher & Sakmann, 1975) and mammals (Cull-Candy *et al.* 1979), it did not describe snake slow fibre synaptic responses.

In addition to the m.e.p.c.s and noise data, a series of voltage-step experiments was performed (Adams, 1974; Dudel, 1978). The step response (Fig. 1*C*) is the difference between currents recorded in the presence and absence of ACh. It illustrates the time course by which the population of channels opened as the old voltage relaxes

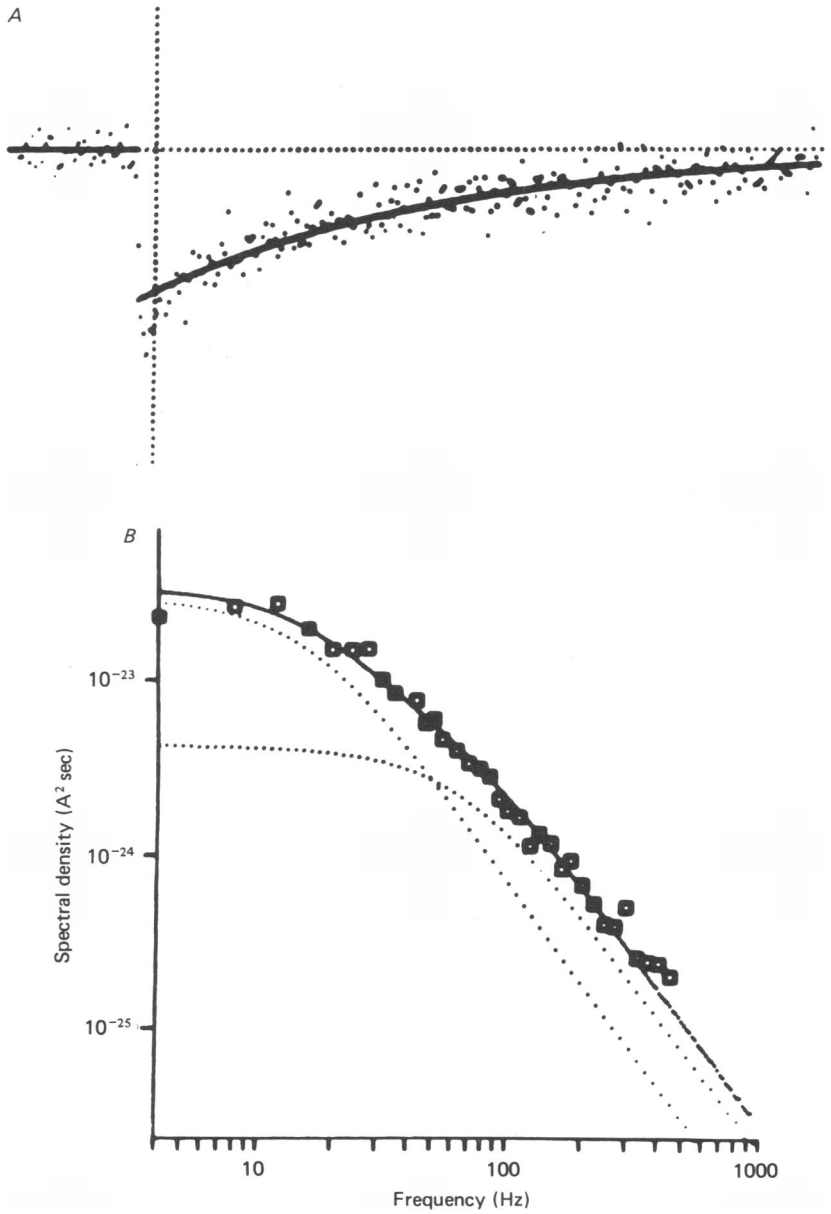

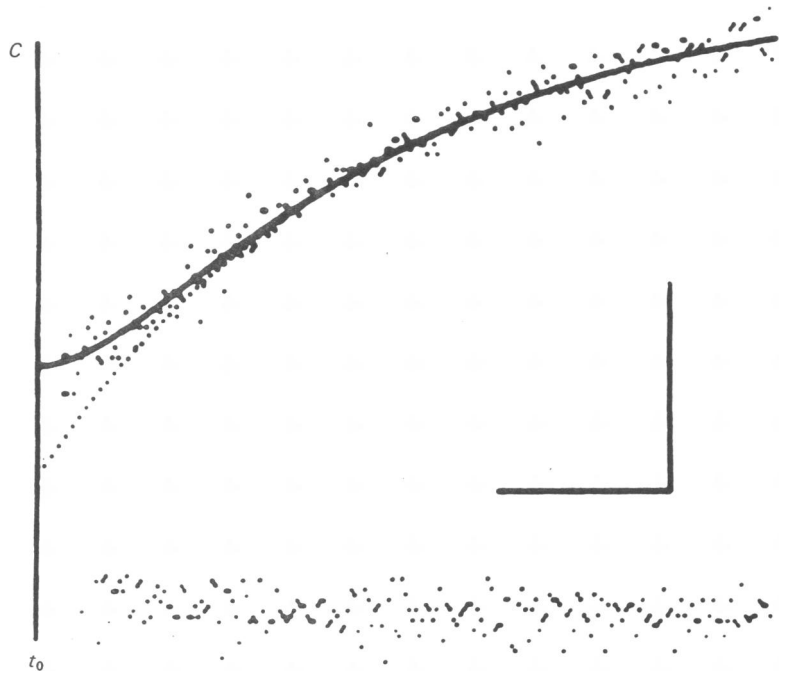

Fig. 1. M.e.p.c., voltage-step current and current fluctuations spectrum from one slow fibre studied at -104 mV, 13 °C. *A*, the average of 5 m.e.p.c.s illustrates the exponential m.e.p.c. time course and its analysis; that portion of the decay after the vertical line was fitted with an exponential curve using a nonlinear least-squares method to determine the m.e.p.c. zero-time amplitude ($-1{\cdot}85$ nA) and decay rate (105 sec^{-1}). Sample interval 100 μsec; 25·4 msec full scale. *B*, two Lorentzian components (dotted lines) were fitted to the spectrum of induced current fluctuations recorded from this cell. The corner frequencies were 17 and 72 Hz, the lower value set equal to the m.e.p.c. decay rate. The relative amplitude of the components (7·0) and the higher corner frequency were treated as variables to fit theory to data. Fitted zero-frequency amplitudes: $4{\cdot}19 \times 10^{-23}$ A^2 sec, $5{\cdot}99 \times 10^{-24}$ A^2 sec. Induced mean current $-6{\cdot}0$ nA. The mean single channel conductance from this data was 20·0 pS. *C*, the voltage-step response time course was acquired by applying ACh in a manner identical to that used to obtain the current noise spectrum in *B*. However, during the application of ACh the membrane voltage was hyperpolarized 39 mV for 250 msec before the time indicated by the vertical line (t_0), then returned to the test voltage (-104 mV) at t_0. As the number of open channels relaxed to a new equilibrium level appropriate for the test voltage the induced current decayed. Two responses are shown in this panel. The upper response is the difference between ten averaged traces recorded in the presence of ACh and ten averaged controls recorded before ACh was applied. The lower response is the difference between 10 averaged controls before and again after the exposure to ACh. The flat control difference indicates that the membrane was stable during the experiment. The upper current time course was fitted here by two theoretical curves, an exponential (dotted) with the m.e.p.c. decay rate and the two-component prediction of the KM kinetic scheme using the noise derived rates. The calibration bars are 2 nA and 5 msec. The initial part of the response after t_0 was blanked to obscure the capacity transient.

at the new voltage. The relaxation occurs because the transition rates between open and closed channel states depend on voltage, so that at different voltages the average number of open channels will not be the same. The decay time course reflects the rapidity of the transition rates among kinetic states at the new voltage in the scheme which describes the channel mechanism. Fitted in Fig. 1*C* are two theoretical lines: one has an exponential time course derived according to a two-state kinetic model with a decay rate predicted from m.e.p.c.s recorded in this cell at the test voltage. At times just after the occurrence of the voltage step this line did not accurately predict the data. Deviations like that shown here were always observed in slow fibre step responses when that cell also showed a two-component spectrum. In twitch fibres and those slow fibres which had a one-component spectrum the step response always showed a monoexponential decay with no deviation at early times. The second theoretical line which more accurately describes the response time course was drawn according to the KM three-state model described below. At the bottom of Fig. 1*C*, is a straight line response which is the difference between control step responses recorded before ACh was applied and again after ACh was removed. Its flatness illustrates that the resting membrane conductance did not change during the course of the voltage step experiment. Measurements in which this was not the case were discarded.

The object of this analysis was to determine the simplest kinetic model which accurately described all of the slow fibre synaptic response data. Two technical factors constrained the data and analysis. First, only open states of the receptor could be detected; consequently, the presence of closed receptor states must be inferred from the rates of appearance and disappearance of open receptors. Secondly, the data were obtained over a limited frequency bandwidth. As will become apparent later, this factor may account for the apparent qualitative differences between spectra and voltage step responses recorded from the twitch and slow end-plates. That is, on general grounds one should expect the responses in both fibre types to exhibit two components.

Theoretical framework

Colquhoun & Hawkes (1977) pointed out that the number of basic components which comprise the impulse, step and equilibrium responses will be one less than the number of kinetic states. Thus, synaptic responses more complex than a single component can be produced in principle if the underlying mechanism has three states or more. For example, if there were three distinct states of the receptor, both the impulse response (m.e.p.c.) and the voltage-step response would be the sum of two exponentials having different decay time contants $\tau_{1,2}$, while the equilibrium response (noise) spectral shape would be the sum of two Lorentzian components with different corner frequencies $f_{1,2}$. The impulse, step and equilibrium responses would remain simply related in the low concentration limit by $f_1 = 1/2\pi\tau_1$ and $f_2 = 1/2\pi\tau_2$. Thus these four parameters would be described by two characteristic values of the particular three-state scheme. These *eigenvalues* are functions of the transition rates which relate the three states to one another, and the general properties of the responses described by them hold although one observes directly only the population of one state, the open channel. A similar description could be made if the responses were

due to four or more distinct states of the receptor but then the number of response components would be greater.

Of the slow fibre spectra 60 % did not have a single Lorentzian line shape; these spectra could be adequately fitted by the sum of two Lorentzian components (Fig. 1). In all cases the two components had corner frequencies which were not widely separated (typical frequency ratio of 4–6), so that their sum was not a curve with two readily distinguished bumps. Instead, the transition region between flat low frequency and $1/f^2$ high-frequency behaviours was broadened compared to the Lorentzian shape.

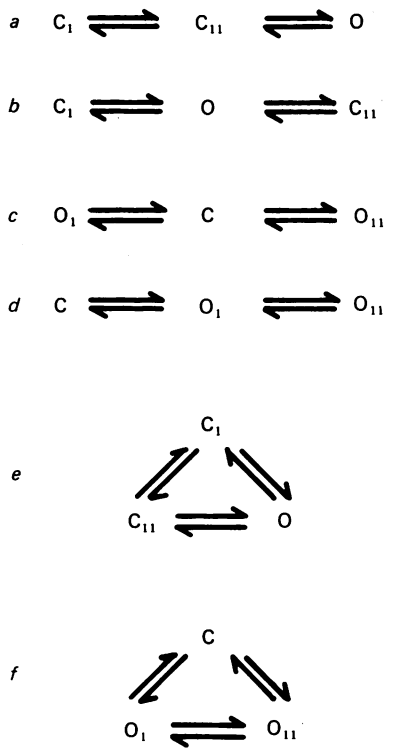

Fig. 2. The general class of three-state kinetic schemes containing both open (O) and closed (C) states. Models from this class were tested for their ability to account for the slow synaptic responses.

Although it is clear that the data require a kinetic model with more than two states for its description, and also that three states are sufficient within the present degree of measurement accuracy, additional states might exist whose effects on the responses were not detected. Models with kinetically undetectable states were formally (if not in fact) excluded from consideration by limiting the analysis to kinetic schemes with three kinetically apparent or distinguishable states. Furthermore, at least one state had to represent an open channel and one a closed channel. Within the class so defined there are six general members (Fig. 2). These six models may be divided into three two-member groups according to the number of free variables in each model. The sequential models with two closed states (Fig. 2*a*, *b*)

contain the minimum number of variables: subclass I. In contrast, the sequential models with two open states have one additional variable, the relative conductance of the open states: subclass II. The cyclic models have one (*e*) or two (*f*) additional variables: subclass III.

In the section on Specific Kinetic Models which follows, both subclass I models will be tested. Each will be presented in the guise of a mechanism which might conceivably account for the responses. Thus Fig. 2 scheme (*a*) is the KM model (Colquhoun & Hawkes (1977) terminology) of del Castillo & Katz (1957) which allows the channel to flutter between open and closed states when the receptor is occupied, and scheme (*b*) is the Blocking model in which the open channel may be transiently blocked. Two special examples of scheme (*c*) will be tested. First is the Two-Agonist Molecule model invoked by Dionne *et al.* (1978) to account for their dose–response work. This model allows channels to open with either one or two bound agonist molecules. Secondly is a model in which there are two adjacent but physically separate populations of cholinergic receptors with different mean lifetimes, synaptic and extrasynaptic channels. Two other mechanisms which were not supported by the data were considered by Dionne & Parsons (1981) when characterizing the slow fibre synaptic response; these were (i) separate populations of Na-selective and K-selective end-plate channels and (ii) separate populations of synaptic and extrasynaptic channels. Both mechanisms may be described by special examples of kinetic scheme (*c*) and a variation of (i) by a special example of kinetic scheme (*d*), but they are defined in such a way that they may be tested on the basis of properties essentially independent of the specific kinetic model (Dionne, 1979). The cyclic models in subclass III were not tested because their extra free variables could not be constrained by the data. Accurate evaluation of any particular transition rate or state lifetime would not be possible with the additional one or two variables these models offered.

In order to test the accuracy of the models, their quantitative predictions were compared with measured responses. These predictions were made with the assumption of low ACh concentration relative to its equilibrium dissociation constant for the receptor. This assumption appears valid because under identical conditions the total noise variance was found proportional to mean end-plate current at constant voltage (Dionne & Parsons, 1981), a linear dependence that should hold only at low concentration.

The mathematical derivation of the expressions appearing below was resonably straightforward. (1) The impulse responses (m.e.p.c.s) were computed by convolving a delta function representing the time course of agonist concentration with the differential equations relating the states of a given kinetic model. Thus, one can write

$$[\text{Agonist}] = c(t) = c_p\delta(0),$$

where c_p is the peak agonist concentration, and the delta function is nonzero only at $t = 0$ where it assumes a value of unity. Although this description is conceptually easy to understand, it does not produce a solution with the correct units. The problem is that we need to deal with the amount of agonist released (per unit volume) rather than its concentration. However, the concept of the peak concentration is important

because some of the arguments assume concentration is small compared to the equilibrium dissociation constant for agonist binding. In order to correct the units and to preserve the identity of the peak agonist concentration, it is useful to describe the amount of agonist released by the impulse as

$$A = c_p \epsilon \text{ (units: M·sec)}$$

where ϵ is a vanishingly small time. A further complication for the units of A will appear when the blocking and KM kinetic models are considered. In these models the binding of a unspecified number of agonist molecules to the receptor is represented by a single transition. In these cases A has the units M^n·sec. An alternative accounting of A can be obtained if one assumes a specified but brief time course for cleft agonist concentration; A is then the integral of the concentration–time relation. This description of A will be useful in the discussion section where the effect of local saturation of slow fibre receptors is considered. (2) The voltage-step responses were predicted by solving the same set of differential equations obtained for the impulse responses, except that concentration was now constant while the voltage-step caused a new value of the transition rates to apply. (3) The temporal behaviour of end-plate current fluctuations could be predicted by computing the correlation function and Fourier transforming it to obtain the spectral density as a function of frequency (Colquhoun & Hawkes, 1977).

Experimental tests among specific kinetic models

There are two fundamentally different ways to model the slow fibre synaptic responses which have been described. First, there might be two types of receptors; several of the models treated here and in Dionne & Parsons (1981) are of this type. Alternatively, all the receptors may be of one type, behaving according to a complicated kinetic scheme. Models of this type also appear herein. The first three sections below describe experimental tests which argue that the slow fibre responses do not arise from either extrasynaptic receptors, channels which open when one or two agonist molecules bind, or a blocking mechanism. The fourth section describes the KM model and shows that it does predict the measured responses.

Extrasynaptic receptors do not account for the observations. It was indicated above that the results might be expected from a mechanism which postulates two physically separate populations of receptors, junctional and extrajunctional. Only the junctional receptors would detect nerve released ACh, so only they could respond during the m.e.p.c., while both junctional and extrajunctional populations would be exposed to ionophoretically released ACh. This could produce the two-component spectra observed if the extrajunctional population had a slightly shorter mean open channel lifetime than the junctional receptors. Receptors in both populations need only obey the simple two-state kinetics of twitch fibre receptors. Dionne & Parsons (1981) tested this model in part; they looked at regions of the muscle far from the end-plate to see if a detectable population of extrasynaptic receptors existed there. None were found. However, that does not preclude the existence of a population of extrajunctional receptors restricted to the immediate vicinity of the end-plate. This mechanism was tested with voltage step experiments.

The synaptic responses for the extrasynaptic mechanism are predicted by kinetic scheme (1).

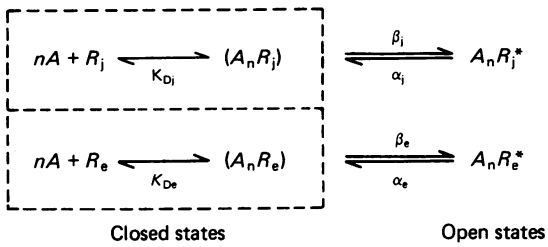

(1)

Here the junctional (j) and extrajunctional (e) receptor populations remain independent of one another. However, the binding of n agonist molecules A to the receptors R to produce the intermediate closed states (A_nR) was assumed to be at equilibrium on the time scale of opening and closing the channels. Within each population of receptors the closed states then become kinetically indistinguishable and the model is reduced to a pair of independent two-state schemes. Under the conditions of the experiment these schemes behave formally like a single three-state model with a common set of closed states.

For this scheme the induced e.p.c. following a voltage-step at time zero will decay according to the following equation.

$$I_E(t) = (V - V_r)\,[(g_j^\infty + \Delta g_j e^{-\alpha_j t}) + (g_e^\infty + \Delta g_e e^{-\alpha_e t})]. \tag{2}$$

The conductance increments are

$$\Delta g_{j,e} = g_{j,e}^0 - g_{j,e}^\infty = G(c, N_{j,e})\left[\frac{\beta_{j,e}^0}{\alpha_{j,e}^0 K_{Dj,e}^0} - \frac{\beta_{j,e}^\infty}{\alpha_{j,e}^\infty K_{Dj,e}^\infty}\right],$$

where 0 identifies the pre-step membrane voltage and ∞ the post-step voltage. Both the initial and final conductance terms $g_{j,e}^0$, $g_{j,e}^\infty$ are functions of the ACh concentration c, the number of available receptors $N_{j,e}$, and the transition rates for the respective populations at the appropriate membrane voltage. The observed transition rates equal the rates of closure of the junctional and extrajunctional channels. Before this e.p.c. time course may be qualitatively described, one must know whether the conductance increments induced by the voltage step add to or subtract from the pre-step conductance values.

According to scheme (1) membrane voltage presumably affects the amplitudes of the observed transitions largely through the rates $\alpha_{j,e}$, while $\beta_{j,e}$ and $K_{Dj,e}$ exhibit little or no voltage sensitivity (Magleby & Stevens, 1972*a*, *b*; Gage & McBurney, 1975; Dionne & Stevens, 1975; Sheridan & Lester, 1977). To the extent that the hypothesized extrajunctional receptors share this property with the junctional receptors (Neher & Sakmann, 1976; Gage & Hammill, 1980), we can write

$$\Delta g_{j,e} = G(c, N_{j,e})\,\frac{\beta_{j,e}}{K_{Dj,e}}\left[\frac{1}{\alpha_{j,e}^0} - \frac{1}{\alpha_{j,e}^\infty}\right]$$

because the pre- and post-step voltages should not alter $\beta_{j,e}$ or $K_{Dj,e}$. Thus, the voltage step will cause the magnitude of the channel closing rates to change, and, most importantly, the direction of this change will determine the sign of the induced

change in mean conductance. For example, if $\alpha^{\infty}_{j,e} > \alpha^{0}_{j,e}$ then $\Delta g_{j,e} > 0$, indicating that $g^{0}_{j,e} > g^{\infty}_{j,e}$; that is, the mean conductance of each population would decrease with the voltage step. However, if the voltage dependencies of the junctional and extrajunctional observed rates were opposite, then one conductance would increment while the other was decremented by the voltage step.

The voltage dependencies of the fitted fast (A_{r_1}) and slow (A_{r_2}) spectral components were estimated from data on six different slow muscle fibres to determine whether Δg_j and Δg_e in eqn. (2) were incremental or decremental changes. These coefficients appear in Table 2 and this data is discussed in more detail later. In every case both fast and slow fitted spectral corner frequencies increased with depolarization; the average slow component changed e-fold in 106 mV, the average fast component in 149 mV. These values indicate that a depolarizing voltage-step experiment, as conducted here, should cause both Δg components to decrement. Thus eqn. (2) describes a time course where the e.p.c. relaxes as the sum of two exponential components from an initial value $I(0)$ to a final value $I(\infty)$. The two components are independent with negative amplitudes, so that the current should exhibit a rapid decay from an initial peak followed by a later, slower declining phase. One test for the adequacy of the model is whether or not such a time course is observed.

The response from a voltage-step experiment is shown in Fig. 1*C*. Note that qualitatively the response time course is not described by eqn. (2). If it were, the current values just after the voltage-step would have been more negative than the fitted single exponential line, not less negative. Although the illustrated deviation of the data from a single exponential is small, it is not artefactual for it was not observed in twitch fibres or slow fibres with a dominant single spectral component and is in the wrong direction to be accounted for by an extrajunctional population of cholinergic channels. The second theoretical line in Fig. 1*C* was predicted by the KM kinetic model (below); not all three-state schemes give the wrong time course for the voltage-step response.

The voltage-step result illustrated in Fig. 1*C* was typical of the slow fibres studied. Seventeen cells with two-component spectra were carefully examined by this method. In no case were the voltage-step response time course deviations from a single exponential in the manner expected from eqn. (2). In all seventeen cells any systematic deviation from exponentiality was in the opposite direction.

The relation between theory and experiment illustrated here is evidence that although two components are present in both the noise and step responses of most slow fibres, they are not produced by separate populations of junctional and extrajunctional receptors.

The Two-Agonist Molecule model does not work. Kinetic scheme (3) describes the binding of two molecules of agonist each with its own equilibrium dissociation constant ($K_1 = k_{10}/k_{01}$; $K_2 = k_{21}/k_{12}$).

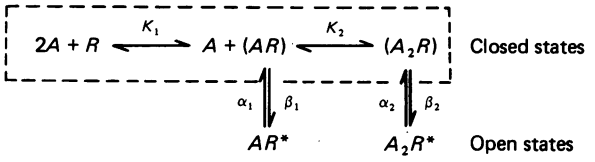

(3)

This scheme has been used to account for dose–response results from frog twitch fibres in which the low concentration Hill slope was between one and two (Dionne *et al.* 1978). Although expressed differently, it was originally treated by Karlin (1967) and later Thron (1973) and Colquhoun (1973). According to scheme (3) either or both agonist binding sites may induce the transition to the open channel state following occupation by agonist. Most commonly, both binding sites would be occupied before the channel opened, but the possibility of a channel opening with only one site occupied is not zero. Rather, using carbachol, this latter probability was estimated at $\sim 1\,\%$ of that for opening produced by two bound agonist molecules (Dionne *et al.* 1978). In applying the Two-Agonist Molecule scheme to slow fibre synaptic responses, it was assumed that the A_2R^* state was the dominant open channel species. The conclusion established below that this model cannot describe the data is independent of this assumption.

The five-state TAM model (3) was truncated to a three-state scheme by assuming the agonist binding and unbinding transition rates were rapid compared to the open-close transition rates. This assumption makes all the closed states in the dashed box kinetically indistinguishable. The two open channel states are produced by transitions out of this set of closed states, these transitions representing conformational changes of the channel proteins.

With this assumption the model predicts an impulse response decay time course (m.e.p.c.) having two exponential components.

$$I_{\mathrm{TAM}}(t) = [g_1(0)\mathrm{e}^{-\alpha_1 t} + g_2(0)\mathrm{e}^{-\alpha_2 t}]\,(V - V_{\mathrm{r}}) \tag{4}$$

where the exponential decay rates are the individual channel closure rates and V_{r} is the reversal potential. It is important to note that this decay time course is accurate only during the decay phase when free agonist concentration is zero. Several time dependent terms decaying as $\exp(-k_{21}t)$ and $\exp(-k_{10}t)$ have been omitted because the assumption of rapid binding means these terms should be rapidly decaying and not resolved on the time scale determined by α_1 and α_2. Consequently, the peak conductances $g_1(0)$ and $g_2(0)$ are values appropriate to back-extrapolation of the decay time course and may not be accurate predictions of the $t = 0$ conductances.

$$g_1(0) = \frac{N\gamma_1\beta_1 A}{K_1}(1 + k_{12}A), \quad g_2(0) = \frac{N\gamma_2\beta_2 A^2 k_{10}}{K_1 K_2}.$$

Here N is the total number of channels, A is the amount of agonist released by the impulse (M·sec), and γ_i is the single channel conductance appropriate for the subscript. Experimentally only the α_2 component was observed in the m.e.p.c. Effectively this means that the ratio $g_1(0)/g_2(0)$ must be much less than unity. Although this description is consistent with the data, the predicted ratio of these peak conductances contains variables which could not be independently evaluated, so that this expression could not be fitted to the data to test the model. The temporal properties of two other types of synaptic response, end-plate current fluctuations and voltage-step, can also be predicted from the TAM model, and both of these can be tested experimentally.

The TAM expression for the spectral density as a function of frequency f is given by

$$S_{TAM}(f) = \frac{S_1(0)}{1+\left(\frac{2\pi f}{\alpha_1}\right)^2} + \frac{S_2(0)}{1+\left(\frac{2\pi f}{\alpha_2}\right)^2}, \tag{5}$$

where the coefficients $S_1(0)$ are

$$S_1(0) = \frac{2N\beta_1\gamma_1{}^2(V-V_r)^2c}{K_1\alpha_1{}^2}, \tag{6}$$

$$S_2(0) = \frac{2N\beta_2\gamma_2^2(V-V_r)^2c^2}{K_1K_2\,\alpha_2^2}. \tag{7}$$

The agonist concentration c was assumed both low and uniform. The assumption of uniformity is not necessary to the experimental test but simplifies the expressions. With regard to this spectral description, the TAM scheme could be tested by determining whether the two spectral component zero frequency amplitudes were shifted with agonist concentration as predicted. According to expressions (6) and (7), $S_1(0) \propto c$ while $S_2(0) \propto c^2$. Thus the spectral frequency amplitude ratio $S_2(0)/S_1(0) \propto c$. If two spectra were recorded, one at just twice the agonist concentration of the other, one would expect that $S_1(0)$ would change by 2 times and $S_2(0)$ by 4 times so that the observed change in the ratio would be 2 times.

For the test experiments it was unnecessary to determine the actual cleft concentration of ACh. Rather, since the scheme limits the dose–response Hill slope to between 1 and 2, it requires that mean end-plate current μ appear to be proportional to concentration to some power $1 < n < 2$. That is, for low concentrations

$$\mu = Kc^n,$$

where K is a constant of proportionality. Kuffler & Yoshikami (1975) measured an n value of 1·8 at garter snake twitch fibre neuromuscular junctions. For the purposes here $c \propto \mu^{1/n}$ and the spectral ratio amplitude is given by

$$R = \frac{S_2(0)}{S_1(0)} \propto \mu^{1/n}.$$

Thus the expression for predicting the spectral ratio R_2 of a second set of data from a measurement of R_1 made on a first set is

$$R_2 = R_1\,(\mu_2/\mu_1)^{1/n}. \tag{8}$$

Qualitatively then scheme (3) predicts that as the mean e.p.c. is increased by raising [ACh], the A_2R^* open channel state should become progressively dominant over the AR^* open channel state. Thus, with increasing μ one should observe a larger spectral ratio. In eight experiments the maximum μ was varied over a range of 2–7 times the minimum, so that depending on the actual n applied here, concentration changes between 2- to 7-fold and 1·4- to 2·7-fold were presumably achieved. The data from the seven cells on which these experiments were performed appear in Table 1. The general trend of the fitted spectral ratio was to remain unchanged with increasing μ, not to reliably increase as predicted by the TAM model. The expected spectral ratio ranges based on eqn. (8) are tabulated for comparison. These data are also plotted

in Fig. 3; first, the range of the ratio predicted by the TAM model was plotted as vertical bars against the fitted ratios. The dashed line in Fig. 3 is the expected locus of points if the model were an accurate representation of the data. It is not. Secondly, the predicted ratios from the general Blocking and KM models (both discussed below) were plotted as points against the fitted ratios in Fig. 3. Both models predict the same values for the spectral amplitude ratio and provide a reasonably accurate description of the data in this test.

TABLE 1. Spectral amplitude ratio *vs.* mean end-plate current

Cell	$V_{membrane}$ (mV)	Mean end-plate Current μ (nA)	Fitted corner frequencies (Hz) Slow	Fast	Spectral ratio fitted	$S_2(0)/S_1(0)$ expected range
19 Dec77.4S	−80	−39·2	21	100	10·6	—
		−76·7			5·9	14·8–20·7
	−100	−40·5	16	64	11·0	—
		−101·5			11·1	17·4–27·6
30 Jan78.2s	−70	−8·5	22	80	3·8	—
		−22·3			4·7	6·2–10·0
30 Jan78.3S	−85	−7·5	26	81	4·7	—
		−20·6			6·7	7·8–12·9
30 Jan78.4S	−70	−9·6	27	132	26·6	—
		−23·2			30·0	41·4–64·3
		−39·7			19·9	54·0–110·0
11 Apr78.7S	−70	−3·0	21	80	10·4	—
		−9·0			5·7	18·0–31·2
		−21·3			3·0	27·7–73·8
26 May78.4S	−61	−3·0	34	135	4·7	—
		−6·0			2·0	6·6–9·4
		−17·2			2·8	11·3–26·9
14 June78.1S	−80	−3·8	21	85	11·4	—
		−6·9			10·0	15·4–20·7
		−9·8			10·0	18·3–29·4
		−22·5			5·4	27·7–67·5

The tabulated data from seven slow fibres (eight voltages) from which spectra were recorded at two or more values of mean e.p.c., μ. The Two-Agonist Molecule model predicts that as μ increases the relative contribution of the AR^* state to the noise current should increase. Thus, one expects the spectral ratio to increase as a predictable function of cleft agonist concentration. Although cleft [ACh] was not measured for technical reasons, the model predicts an allowed range for the spectral ratio which depends on the change in μ. Both the fitted and predicted spectral ratios are tabulated here. The predicted spectral ratio ranges are given for each experiment based upon the fitted ratio for the lowest e.p.c. value. The fitted fast and slow characteristic frequencies of the spectral components are also listed; these values did not depend on [ACh], although they were voltage dependent.

Finally, the shape of the voltage-step response (Fig. 1*C*) provides an independent test which supports a conclusion that the TAM model is inaccurate. The TAM model predicts a step response time course which decays from a zero-time value as the sum of two exponential components, a fast decay with rate α_1 and a slow decay

with rate α_2. Qualitatively the predicted response is similar to that described for the extrajunctional model, so that the TAM model is then just as poor in its prediction of this response. That is, the faster component deviates from the slower component in the direction opposite to that predicted. Thus, both the dependence of the spectral components on concentration and the voltage-step response time course argue that the TAM model cannot describe the ACh-operated channel mechanism in slow fibres.

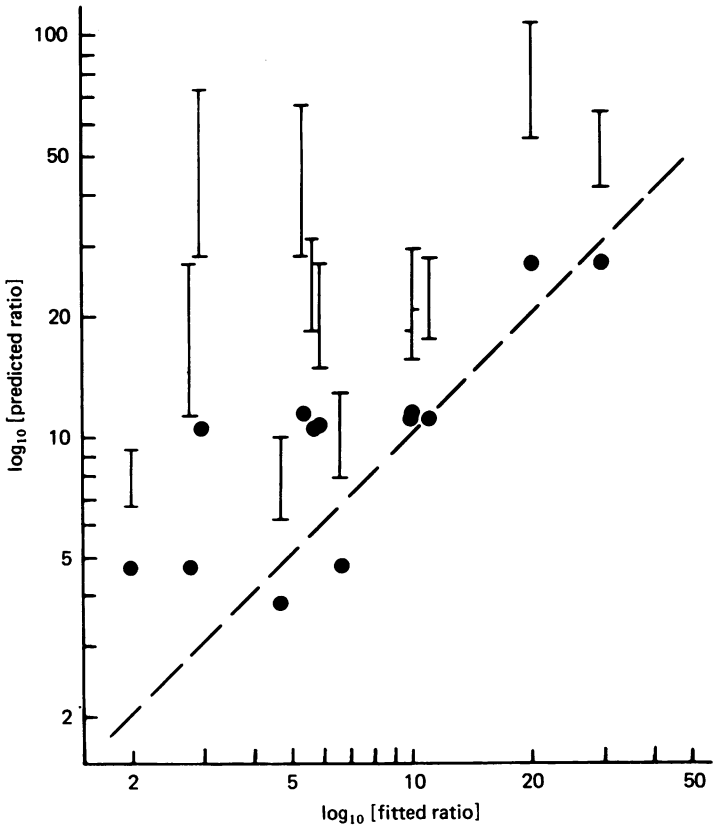

Fig. 3. The dependence of spectral amplitude ratio upon mean end-plate current. The data in Table 1 provided one test of the Two-Agonist Molecule model by plotting the predicted amplitude ratio against the fitted ratio using expression (8). The ranges of predicted values appear as vertical bars; in all cases the predicted range was greater than that fitted (dashed line). For comparison, the predicted ratio values according to either the Blocking or KM models were plotted as dots. These two models predict the same result for this test. The Blocking/KM predictions were always less than the Two-Agonist Molecule predicted range and were distributed along the dashed line of expected values.

The Blocking model does not work. Kinetic scheme (9) describes the binding of an undefined number n of agonist molecules to the receptor to form an intermediate closed state (A_nR). This intermediate can make the transition to open channel A_nR^*, and only the open channel can be blocked to produce the non-conducting state A_nR^0.

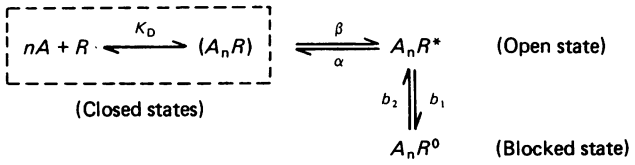

(9)

This four-state model was reduced to three states by assuming again that binding rates were rapid relative to the conformational changes represented by the open-close transitions. Thus the model consists of a pool of kinetically indistinguishable closed states (the dashed box), the open channel state and the blocked channel state. The model gives an impulse response

$$I_B(t) = [g_1(0)\,e^{-r_1 t} + g_2(0)\,e^{-r_2 t}]\,(V - V_r) \tag{10}$$

and noise spectrum

$$S_B(f) = \frac{S_1(0)}{1+\left(\frac{2\pi f}{\omega_1}\right)^2} + \frac{S_2(0)}{1+\left(\frac{2\pi f}{\omega_2}\right)^2}. \tag{11}$$

The parameters in these expressions are related as follows.

Spectral corner frequencies $\omega_i = 2\pi f_i$, $i = 1,2$

$$\omega_{1,2} = 1/2\{b_1 + b_2 + \alpha(c+1) \pm \sqrt{[(b_1 + b_2 + \alpha(c+1))^2 - 4\alpha b_2 d]}\}.$$

Impulse decay rates $r_1 = \omega_1\,(c = 0)$

Amplitudes

$$g_1(0) = \frac{\beta AN}{K_D}\left(\frac{b_2 - r_1}{r_2 - r_1}\right),$$

$$g_2(0) = \frac{\beta AN}{K_D}\left(\frac{r_2 - b_2}{r_2 - r_1}\right).$$

$$S_1(0) = 4N\gamma^2(V - V_r)^2\left(\frac{cb_2}{d^2\omega_1(\omega_1 - \omega_2)}\right)\frac{(\alpha c/b_2 - 1)(1 - \omega_1/b_2)}{(1 - \alpha c/\omega_2)},$$

$$S_2(0) = -4N\gamma^2(V - V_r)^2\left(\frac{cb_2}{d^2\omega_2(\omega_1 - \omega_2)}\right)\frac{(\alpha c/b_2 - 1)(1 - \omega_2/b_2)}{(1 - \alpha c/\omega_1)}.$$

Coefficients

A = amount of agonist released at impulse (units: $\text{M}^n\cdot\text{sec}$),

$$c = \frac{\beta[\text{A}]^n}{\alpha(K_D + [\text{A}]^n)}, \quad [\text{A}] \text{ assumed uniform},$$

$$d = 1 + c(1 + b_1/b_2).$$

Inspection of the expressions for r_i, the apparent decay rates at zero [ACh], reveals that r_1 is always the faster rate and r_2 always the slower. As indicated above, the Blocking model predicts that the zero frequency amplitudes of the two spectral components $S_i(0)$ depend identically on concentration so that a shift in mean e.p.c. will produce no change in spectral shape. Thus the Blocking model performs satisfactorily in this test which ruled against the TAM model. Furthermore, depending

upon the charge properties of the (endogenous?) Blocking molecule, the time course of the voltage-step response can be made to mimic that shown in Fig. 1*C* (Adams & Sakmann, 1978*a*). However, another test can be formulated for this model which it fails.

At low agonist concentrations the model provides a relation between the ratio of the m.e.p.c. component amplitudes and the spectral amplitudes. The m.e.p.c. amplitude ratio $g_1(0)/g_2(0)$ can then be predicted from the zero frequency amplitudes $S_i(0)$ and corner frequencies f_i of the spectrum. If the Blocking model is to be successful it must predict a small amplitude for the higher frequency impulse component $g_1(0)$ because only the lower frequency component was observed. The following expression relates the normalized high frequency impulse amplitude to the spectra at low concentration.

$$\frac{g_1(0)}{g_2(0)} = \frac{f_1}{f_2}\frac{S_1(0)}{S_2(0)}. \tag{12}$$

To test this dependence 59 paired m.e.p.c. averages and spectra from thirty-five cells were analysed. On the basis of eqn. (12) the spectral data predicted a range for the m.e.p.c. amplitude ratio of $0{\cdot}14 \leqslant g_1(0)/g_2(0) \leqslant 2{\cdot}94$ with a mean value of $0{\cdot}52 \pm 0{\cdot}48$ (59). The maximum acceptable values for the amplitude ratio were determined separately by superimposing on each of the mean m.e.p.c.s a two-component computer-generated 'm.e.p.c.' with the rates derived from the spectrum and an adjustable amplitude ratio. The maximum relative value for the higher frequency component was defined as that which produced no apparent distortion from the declining phase of the m.e.p.c. within the noise envelope of the data record. The range for the maximum amplitude ratio defined in this manner was $0 \leqslant g_1(0)/g_2(0) \leqslant 1{\cdot}21$ with a mean of $0{\cdot}20 \pm 0{\cdot}22$ (59). The maximum fitted m.e.p.c. amplitude ratio for each cell was plotted against the predicted component ratio in Fig. 4. The line at 45° represents the expected curve if the data and theory agreed; they do not. The data in this figure has been further subdivided according to the spectral component ratio. Those cells in which the amplitude of the higher frequency spectral component was greater than 10% of the lower frequency amplitude were plotted as filled circles (●) and the others as open circles (○). Miniature e.p.c.s from cells having a dominant two-component spectral character have a larger predicted m.e.p.c. amplitude ratio but do not have a correspondingly large fitted amplitude ratio. One must conclude that the Blocking model cannot account for the two-component character of the slow fibre synaptic response.

This method of testing the Blocking model used observed rates estimated from the spectra to predict the expected ratio of the m.e.p.c. amplitude components. As pointed out above, the spectral rates were evaluated under conditions of low ACh concentration; however, it is plausible that the m.e.p.c. peak amplitude occurred when the local ACh concentration was quite large (Kuffler & Yoshikami, 1975). Thus, the low concentration rates might not be appropriate to predict the m.e.p.c. amplitude ratio. Yet it would appear that expression (12) gives a lower bound for the amplitude ratio; as agonist concentration is increased, and possibly prolonged for a few tens of microseconds both apparent rates should increase. The faster component of the m.e.p.c. should decay more rapidly from a relatively larger peak.

Thus, while the test as outlined may not be accurate, it does provide a useful limit. Discrepancies which could arise associated with agonist concentration would appear to exaggerate the predicted m.e.p.c. amplitude ratio in a manner to make it more difficult for the data to be accurately described by the Blocking theory.

An important variation of the Blocking model occurs when the agonist itself becomes the blocking agent. For example, decamethonium appears to both activate the ACh-operated channel and block it (Adams & Sakmann, 1978*a*). If ACh functioned in a similar manner at the snake slow muscle neuromuscular junction, one

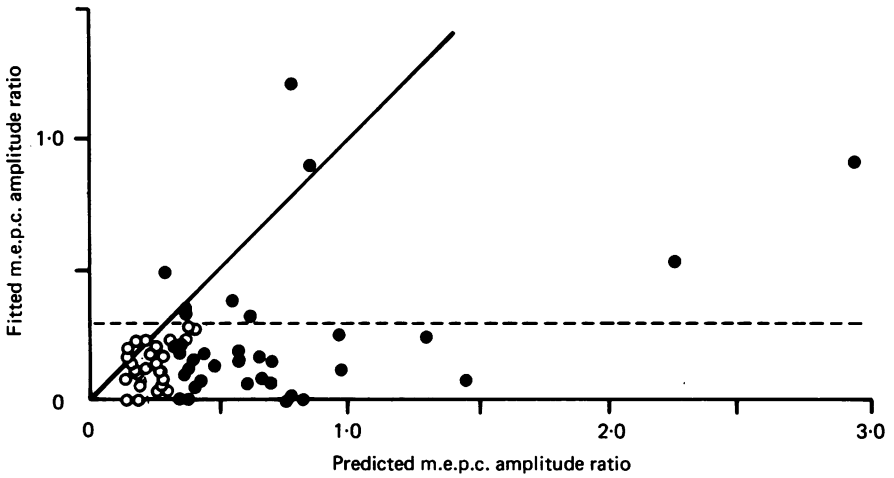

Fig. 4. Predicted m.e.p.c. amplitude ratio from the Blocking model. Averages of twenty or fewer m.e.p.c.s were compared with a two-component computer-generated theory to estimate the maximum relative amplitude of the predicted rapidly decaying initial component, according to the Blocking model. Approximately 8 % of the mean m.e.p.c.s displayed decay phases which were clearly not a single exponential component (see the Discussion of the KM model). In this sample, 15 % of the events appeared to have two components; they plotted above the dashed line, having fitted ratios > 0·3. Eqn. (12) was used to predict the m.e.p.c. component amplitude ratio for each average, and the fitted values were plotted against the predicted values. If the Blocking theory accurately described the results, one would expect the data points to be distributed along the continuous line with a slope of 1. However, the theory was not an accurate reflexion of the data. The data points have been further subdivided: ○ ≡ higher frequency spectral component amplitude < 10 % of the lower frequency component, amplitude; ● ≡ ≥ 10 %. Dominance in the spectra of two components did not correlate well with the presence of two m.e.p.c. decay components.

could predict qualitatively the synaptic responses observed. Furthermore, this model might not be ruled out by the test described above, because the blocking substrate would be present only briefly during the m.e.p.c. However, systematic changes of m.e.p.c. amplitude and both the spectral ratio and the fitted characteristic frequencies would be expected from this mechanism as would changes in the voltage-step response. These predicted changes depend upon agonist concentration (Adams & Sakmann, 1978*a*). First, no depression of m.e.p.c. peak amplitude or alteration of m.e.p.c. time course was noticed when m.e.p.c.s were recorded during ionophoretic application of ACh. Secondly, if the forward blocking rate $b_1 = b[\mathrm{ACh}]$, then the

TABLE 2. Voltage-dependent coefficients of the KM derived parameters

Cell	No. of voltages	A_α ($-A_{r_1}$)	A_{τ_2}	A_β	A_{k_2}	A_{r_1}	A_{r_2}
25 Nov77.2S	4	0·0058 (0·96)	−0·0056 (0·99)	0·0063 (0·72)	0·0054 (1·00)	0·0058 (1·00)	0·0054 (1·00)
15 Dec77.3S	3	0·0030 (1·00)	−0·0075 (0·99)	0·0028 (0·50)	0·0105 (0·97)	0·0049 (1·00)	0·0088 (0·99)
19 Dec77.4S	5	0·0098 (0·80)	−0·0085 (0·78)	0·0082 (0·99)	0·0087 (0·66)	0·0086 (0·91)	0·0095 (0·79)
22 Dec77.4S	3	0·0016 (0·91)	−0·0057 (0·66)	0·0077 (0·68)	0·0042 (0·66)	0·0071 (0·87)	0·0086 (0·96)
9 Aug78.4S	4	0·0079 (0·98)	−0·0100 (0·93)	0·0001	0·0145 (0·92)	0·0078 (0·99)	0·0144 (0·99)
10 Aug78.4S	5	0·0066 (0·98)	−0·0069 (0·98)	0·0003	0·0094 (0·96)	0·0060 (0·99)	0·0100 (0·99)
Means ± S.D.		0·0075 ± 0·0030	−0·0074 ± 0·0017	0·0042 ± 0·0037	0·0089 ± 0·0037	0·0067 ± 0·0014	0·0095 ± 0·0029

In the six cells listed here data at three to five voltages were obtained and used to evaluate the transition rates of the KM kinetic scheme. This Table lists the coefficients of voltage dependence (units: mV^{-1}) for the derived parameters α, τ_1, τ_2, β, k_2 as well as the apparent rates r_1 and r_2. The value in parentheses is the coefficient of determination of the regression lines, fitted as in Fig. 5.

equations describing the spectral response predict that increasing [ACh] should result in increasing the faster observed frequency r_1 while decreasing both the slower observed frequency r_2 and the spectral ratio $S_2(0)/S_1(0)$. Experimentally, however, the observed frequencies appeared to be independent of [ACh] (see Table 1) while the spectral ratio displayed no reliable concentration dependence. Although uncertainties in the data may have obscured the predicted concentration dependencies, this data does not support the self-block mechanism.

The KM model works. Kinetic scheme (13) describes the binding of an unspecified number of agonist molecules to a channel-receptor to produce the closed intermediate state (A_nR). This intermediate may undergo a reversible conformational transition to create the open channel state A_nR^*.

$$nA + R \underset{k_2}{\overset{k_1}{\rightleftharpoons}} (A_nR) \underset{\alpha}{\overset{\beta}{\rightleftharpoons}} A_nR^*. \tag{13}$$

The KM scheme contains three states, and no assumptions on the relative magnitudes of the rates are required to truncate it. However, the physical meaning of the binding and unbinding transitions is obscured by the possibility that n may not be unity and may even be non-integral. The model predicts a two-component impulse response:

$$I_{KMI}(t) = I_{KM}[e^{-r_2 t} - e^{-r_1 t}] \tag{14}$$

a two-component noise spectrum:

$$S_{KM}(f) = \frac{S_1(0)}{1 + \left(\frac{2\pi f}{\omega_1}\right)^2} + \frac{S_2(0)}{1 + \left(\frac{2\pi f}{\omega_2}\right)^2} \tag{15}$$

and a two-component voltage-step response:

$$I_{KMJ}(t) = I(\infty) + \frac{I(0) - I(\infty)}{\omega_2 - \omega_1} [\omega_2 e^{-\omega_1 t} - \omega_1 e^{-\omega_2 t}]. \tag{16}$$

The parameters appearing in these equations are related to the transition rates as follows.

Step decay rates and spectral corner frequencies:

$$\omega_i = 2\pi f_i, \quad i = 1,2$$

$$\omega_{1,2} = \tfrac{1}{2}\{\alpha + \beta + k_2 + c^n k_1 \pm \sqrt{[(\alpha + \beta + k_2 + c^n k_1)^2 - 4\alpha k_2 d]}\} \tag{17}$$

Impulse decay rates:

$$r_i = \omega_i \Big|_{c=0}.$$

Amplitudes:

$$I_{KM} = \frac{k_1 \beta A N \gamma (V - V_r)}{(r_1 - r_2)},$$

$$S_1(0) = -\frac{4Nc^n \beta \gamma^2 k_1 (V - V_r)^2 (\alpha - \omega_2)}{k_2 \alpha d^2 \omega_1 (\omega_1 - \omega_2)(1 - k_1 c^n/\omega_2)},$$

$$S_2(0) = \frac{4Nc^n\beta\gamma^2k_1(V-V_r)^2\,(\alpha-\omega_1)}{k_2\alpha d^2\omega_2(\omega_1-\omega_2)\,(1-k_1c^n/\omega_1)},$$

$$I(j) = \frac{\beta_1k_{1j}c^nN}{k_{1j}c^n(\alpha_j+\beta_j)+k_{2j}\alpha_j} \quad (j = 0 \text{ before step, } \infty \text{ after}).$$

Coefficients:

A = 'amount' of agonist released at impulse (units $\text{M}^n\cdot\text{sec}$).

c = [ACh],

$$d = \frac{c^nk_1(\alpha+\beta)}{k_2\alpha}+1.$$

The KM kinetic scheme yields a predicted m.e.p.c. that decays as a single exponential function of time (Fig. 5*A*). In the notation of eqn. (14) it has the decay rate r_2. The additional component with rate r_1 largely accounts for the rising phase and the time-to-peak of the m.e.p.c. The two components have identical amplitudes with opposite signs so that at $t = 0$ the m.e.p.c. amplitude is zero. These are just the properties of the common slow fibre m.e.p.c.s (Dionne & Parsons, 1981). According to eqn. (14) the peak current will be measurably delayed after the concentration impulse at time zero. Estimates of time-to-peak can be obtained from the data and compared with the theory; they will be discussed below.

The KM kinetic scheme predicts two-component spectra in contrast to the single-component m.e.p.c. decay (Fig. 5*B*). The relative amplitudes of the spectral components are (slow/fast)

$$\frac{S_2(0)}{S_1(0)} = \frac{\omega_1(\omega_1-\alpha)\,(1-k_1c^n/\omega_2)}{\omega_2(1-k_1c^n/\omega_1)\,(\alpha-\omega_2)}.$$

At low concentrations ($c \ll k_2/k_1$) this reduces to

$$\frac{S_2(0)}{S_1(0)} = \frac{r_1(r_1-\alpha)}{r_2(\alpha-r_2)}, \tag{18}$$

which is independent of agonist concentration. Thus different concentrations of agonist will not cause the spectral shape to change although the mean current and the total current variance will be altered because different numbers of channels will be opened. This preduction is in accordance with the data (see Table 1) and is one point on which the TAM model failed.

Finally, the KM-predicted voltage-step response time course exhibits two exponential components (eqn. (16), Fig. 5*C*). At longer times after the step the response is essentially a single exponential decay with rate r_2, the same rate as the m.e.p.c. decay phase. Shortly after the step, however, the currents are described by the sum of two rates whose combined amplitude is smaller than that of the r_2 component alone. Thus, the voltage-step response should appear as an exponential decay with a rounded peak near $t = 0$. An example of a slow fibre voltage-step response appears in Fig. 1*C*. The rates for the fitted KM time course superimposed on this data were obtained separately from analysis of m.e.p.c.s and noise recorded

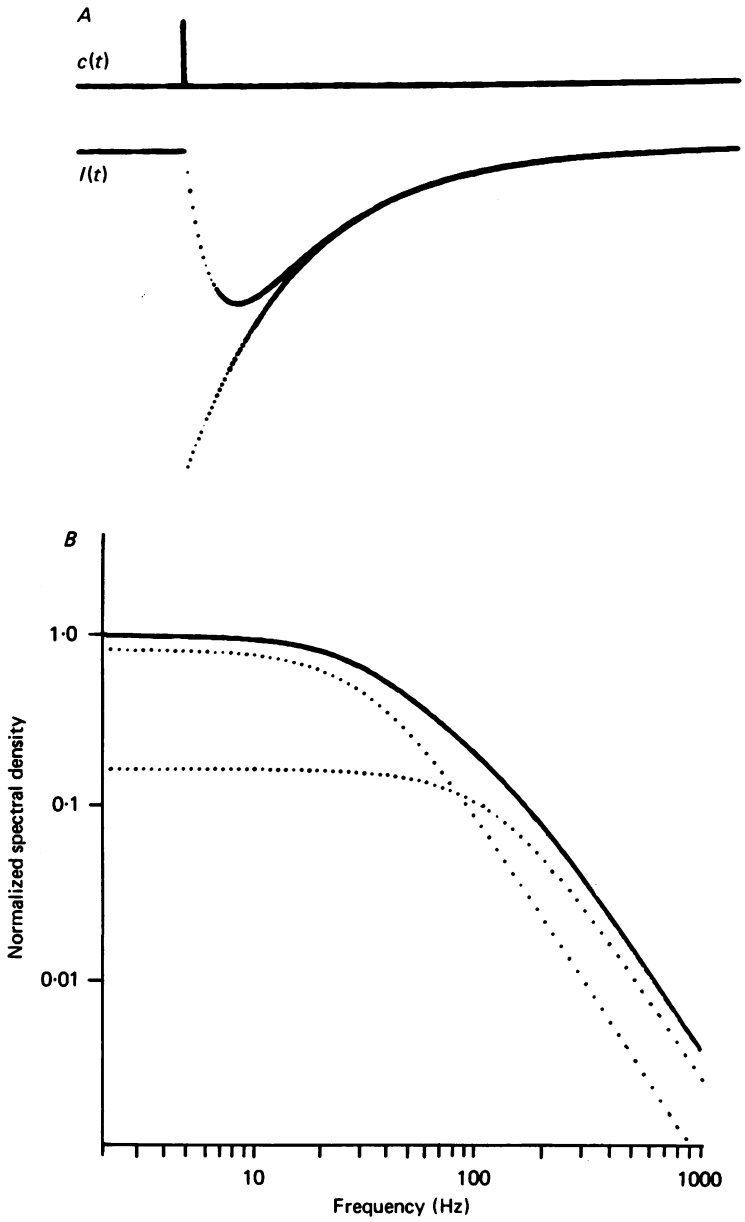

at the same voltage from this cell. Thus, the shape of the time course is accurately predicted by the KM kinetic model. No other kinetic model considered here successfully described the voltage-step response.

DISCUSSION

The KM scheme has been identified as the only three-state kinetic model from among those tested which accurately describes the slow fibre synaptic responses. The data allows three of the four kinetic rates in that model to be evaluated in the

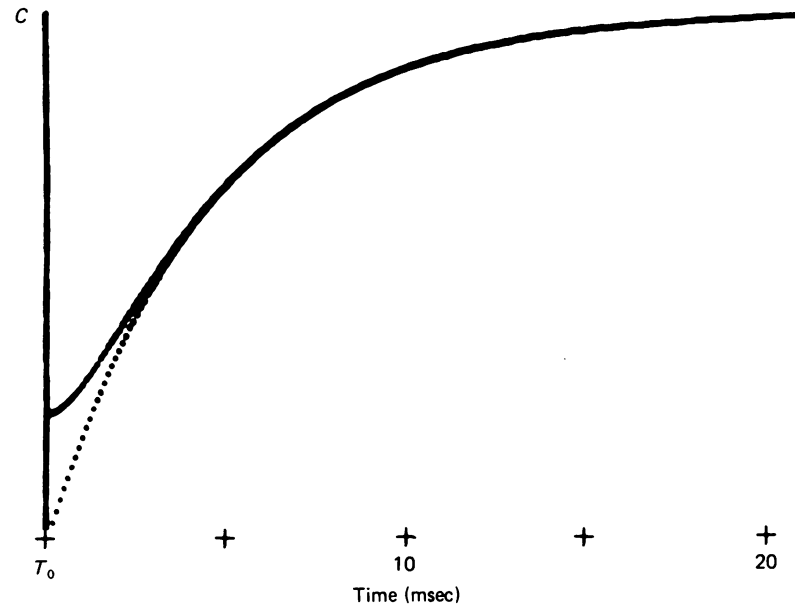

Fig. 5. Predictions of the observed responses according to the KM kinetic scheme. The theoretical responses illustrated here were generated by the KM kinetic model using the following rates: $\alpha = 350\ \text{sec}^{-1}$, $\beta = 200\ \text{sec}^{-1}$, $k_2 = 600\ \text{sec}^{-1}$. These transition rates yield two observable rates using eqn. (17) at low (zero) [ACh]: $r_1 = 922\ \text{sec}^{-1}$ and $r_2 = 228\ \text{sec}^{-1}$. Compare this figure with Fig. 1. *A*, the m.e.p.c. time course is shown superimposed at longer times with the single exponential component of rate r_2. Estimation of the m.e.p.c. decay rate by the methods herein would give r_2 only. The nonsaturating [ACh] pulse used to stimulate the m.e.p.c. is shown above it. Time base: 100 μsec/pt; 25·5 msec total. *B*, the two observable rates are equivalent to Lorentzian corner frequencies of 36 and 147 Hz. These individual components (dotted) and their sum have been plotted with a relative amplitude of five to illustrate that the theory generates spectra like those observed in slow fibres. *C* the predicted voltage-step relaxation is S-shaped; it deviates from a single exponential (rate r_2, dotted) for several msec following the step at T_0, then becomes indistinguishable from the exponential component. Time base: 100 μsec/pt; 5 msec/cursor.

low concentration limit and in terms of them the lifetimes of the two transient states, (A_nR) and A_nR^*, may be given. In addition, the expression for m.e.p.c. time course (eqn. (14)) can be used to evaluate the time-to-peak of the m.e.p.c. These topics will be handled in the two sections below.

Evaluation of the transition rates and state lifetimes. For a given set of experimental conditions the fitted values for $f_{1,2}$ and $S_{1,2}(0)$, obtained from both m.e.p.c.s and noise, can be used to estimate the channel closing and opening rates α and β, and the agonist unbinding rate k_2; the lifetimes of the open channel state τ_1 and the closed intermediate state τ_2 can be expressed in terms of them. From the equations describing the KM model (13) the following expressions may be derived.

$$\alpha = 2\pi\left[\frac{f_1^2+f_2^2(S_2(0)/S_1(0))}{f_1+f_2(S_2(0)/S_1(0))}\right],$$

$$k_2 = 4\pi^2 f_1 f_2/\alpha,$$

$$\beta = 2\pi(f_1+f_2)-\alpha-k_2,$$

$$\tau_1 = \frac{1}{\alpha},$$

$$\tau_2 = \frac{1}{\beta+k_2}.$$

Of the > 100 slow cells studied, both m.e.p.c.s and noise were recorded at three or more voltages from only six cells. Another eleven cells yielded data at two voltages. The derived rates and lifetimes for one cell studied at five voltages were plotted in Fig. 6*A*. These data have been displayed semilogarithmically and fitted with the expression $p_1 = \tilde{p}_1 \exp(-A_1 V)$, where p_1 are the individual rates or lifetimes and A_1 the coefficients of voltage dependence. These coefficients have been tabulated (Table 2) for the six cells with three or more voltage values. The combined data from the fifteen cells studied at two or more voltages was also pooled into six voltage bins and the mean values plotted against voltage in Fig. 5*B*. The voltage-dependent coefficients derived from this figure were essentially the same as the mean values in Table 2.

The following general observations on these results can be made:

Conformational change rates. The channel closing rate α had a nominal value of several hundred per second; it increased with membrane depolarization, changing *e*-fold in about 130 mV. Its magnitude was quite similar to α in twitch fibres although it was somewhat less voltage-sensitive. The magnitude of α was much greater than the m.e.p.c. decay rate, illustrating that the decay of this synaptic event was determined by several kinetic steps, not just channel closure. The opening rate β had a typical value of ~ 220 sec^{-1} and showed the least voltage sensitivity of the derived quantitities. However, a small voltage dependence would not have been well resolved in the data. This channel opening rate is ~ 10 times smaller than Adams & Sakmann's (1978*b*) estimate from frog twitch fibres. Whether the value is physiologically acceptable may be determined by the ratio $\beta/(\alpha+\beta)$ which defines the fraction of channels open at equilibrium (given receptors with bound agonist). At -80 mV and 14 °C approximately 42 % of the slow fibre channels should be open. Although this is less than the 90 % estimated in twitch fibres (Adams & Sakmann, 1978*b*) it would appear satisfactory, especially as slow fibre channels have a greater probability of opening more than once (below).

Unbinding rate. The unbinding rate k_2 was more rapid than either of the conformational change rates, and like α it was voltage-dependent. At -75 mV (14 °C) it averaged about 420 sec^{-1} and increased with depolarization e-fold in about 108 mV. This voltage change parallels that for the channel closing rate, α. At 0 mV membrane potential the expected rate would be $\sim$ 1000 sec^{-1}. The precise physical interpretation of k_2 is not clear. Evidently two molecules of agonist normally bind to the channel receptor before opening can occur; k_2 might then reflect one of several changes during the unbinding process or it might reflect several individual unbinding steps overall.

State lifetimes. Both the open channel lifetime $\tau_1 = 1/\alpha$ and the closed transition-state lifetime $\tau_2 = 1/(\beta + k_2)$ had millisecond values with the open-state lifetime always exceeding the closed-state value. The open channel lifetime τ_1 was similar in magnitude to that described for twitch fibre synaptic channels (Dionne & Parsons, 1981). It increased exponentially with hyperpolarization because it is reciprocally

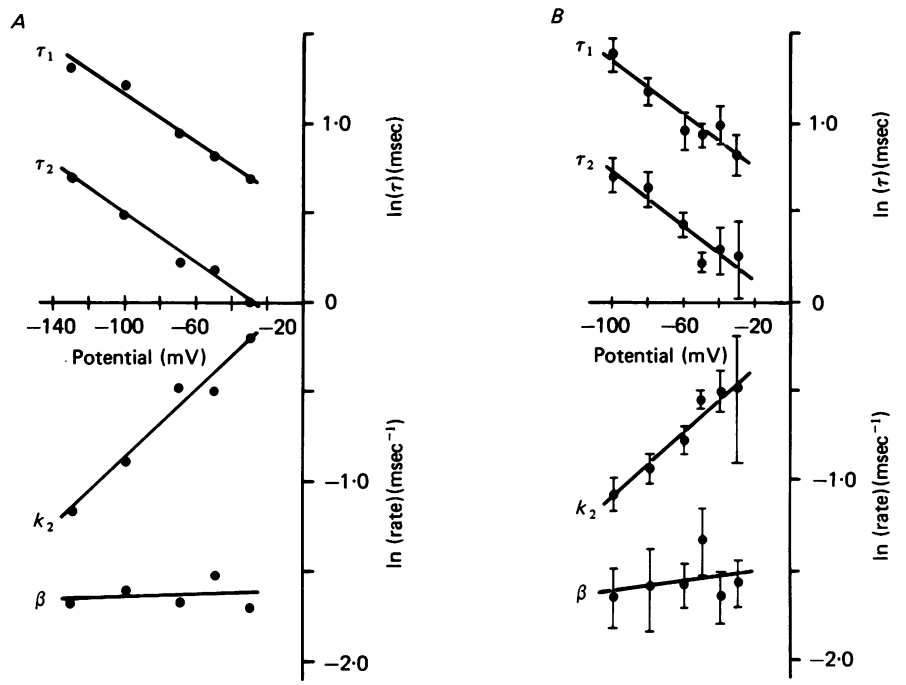

Fig. 6. Voltage dependence of the KM model derived rates. The slow fibre data was fitted with the KM kinetic scheme to estimate the rates α, β and k_2. Plotted here as a function of membrane voltage are β and k_2 and the state lifetimes $\tau_1 = 1/\alpha$ (mean open channel lifetime) and $\tau_2 = 1/(\beta + k_2)$ (mean transition state lifetime). The data from one individual fibre are presented (*A*) along with the pooled data from seventeen cells studied at two to five different voltages each (*B*). Both indicate that the rates $\alpha(= 1/\tau_1)$ and k_2 depend exponentially on voltage, increasing with depolarization, while β showed much less voltage dependence. As described in the Methods, the observable rates r_1 and r_2 were fitted to constrain the variation of β within a cell. Although this fitting procedure would lessen any true voltage dependent change in β, no reliable indication of such a dependence was detected even before the procedure was adopted. In contrast the voltage dependencies of both α and k_2 were evident from the first fitting, and the variation method which controlled β served to increase the confidence levels of the least-squares regression lines fitted to that data. The pooled data in *B* are plotted as mean ± S.E. of mean. The points from −100 to −30 mV represent eight, nine, eight, six, five and two values respectively. Data from these cells were used if they fell within 2 mV of the potentials plotted. These data yielded the following expressions for the least-squares fits.

$\tau_1 = 1{\cdot}80 \exp(-0.0075\ V)$ msec; $\tau_2 = 0{\cdot}95 \exp(-0{\cdot}0076\ V)$ msec; $k_2 = 1190 \exp(0{\cdot}0093\ V)\ sec^{-1}$; $\beta = 230 \exp(0{\cdot}0013\ V)\ sec^{-1}$; $\alpha = 550 \exp(0{\cdot}0075\ V)\ sec^{-1}$. The comparable expressions for *A* appear in Table 2, cell 10AUG78.4S.

related to the closing rate α. The transition state lifetime τ_2 also increased with membrane hyperpolarization, because the unbinding rate k_2 was voltage dependent (although β was not). Experimentally, both τ_2 and k_2 appeared to depend exponentially on V, but because they are nonlinearly related, this cannot be a perfectly accurate description. Nevertheless, it held to within experimental accuracy over the voltage range examined. At -75 mV (14 °C) the average slow fibre channel had an open lifetime of 3·2 msec and a closed intermediate state lifetime of 1·7 msec. Both values appeared to change e-fold in about 130 mV, so that at 0 mV the estimated lifetimes would be: open 1·8 msec, closed 1·0 msec.

Thus the kinetic scheme which describes the averaged synaptic responses recorded from these slow muscle end-plates at 14 °C may be written

$$nA + R \underset{1000 \exp 0{\cdot}0093V \text{ sec}^{-1}}{\overset{k_1}{\rightleftharpoons}} (A_nR) \underset{550 \exp 0{\cdot}0075V \text{ sec}^{-1}}{\overset{220 \text{ sec}^{-1}}{\rightleftharpoons}} A_nR^*,$$

where V is given in millivolts.

Estimation of m.e.p.c. time-to-peak. The time-to-peak of the m.e.p.c.s recorded in this study ranged between 200–600 μsec. Moreover, it was possible that the rise times of the fastest events were limited by the clamp, so that this range of times-to-peak may be biased to longer values. Nevertheless, the following expression derived by differentiation of eqn. (14) predicted t_{peak} values about 10 times *greater* than those observed:

$$t_{peak} = \frac{1}{r_2 - r_1} \ln \frac{r_2}{r_1}.$$

If there were no way to correct this estimate, it would provide a strong argument against either the method of estimation of the observable rates or against the KM kinetic scheme. However, the observed rates should depend on concentration according to eqn. (17) in such a way that as c is increased both observed rates increase. The effect of this concentration dependence on the risetime is dramatic, so that at $c^n = 10K_D$ ($K_D = k_2/k_1$) the m.e.p.c. time-to-peak is reduced to a few hundred μsec, just as observed. This difference is illustrated between Fig. 5*A* and 7*A*. Both figures show simulated m.e.p.c.s derived using the same values for α, β and k_2. In Fig. 5*A* the low agonist concentration limit was used to predict $t_{peak} \simeq 2$ msec, while in Fig. 7*A* maximum $[ACh]^n = 10K_D$ and $t_{peak} \simeq 0{\cdot}5$ msec. This value for the local peak [ACh] following vesicle release does not seem unreasonable (Kuffler & Yoshikami, 1975; Mathews-Bellinger & Salpeter, 1978). Thus the KM kinetic model can reproduce the observed m.e.p.c. rise times and times-to-peak with the estimated transition rates if the peak local [ACh] caused by the release of one vesicle is much larger than the receptor K_D.

The infrequent two-component m.e.p.c.s which were observed can also be accounted for by a temporarily large [ACh] at the m.e.p.c. peak which, in addition, is maintained for a brief but non-negligible time. The simulated m.e.p.c. time courses in Fig. 7 were produced by convolving an exponentially decaying agonist concentration pulse with the differential equations describing the KM model, rather than by using a delta function. Agonist concentration was assumed to rise almost instantly to a peak value of $10K_D$, then to decay in time as $\exp(-t/\tau_A)$. Fig. 7*A* differs

from 7*B* only in the value of τ_A that was assumed. In 7*A* [ACh] decayed with a characteristic time of about 250 μsec; in Fig. 7*B* the value was 500 μsec. In Fig. 7*B* with the prolonged [ACh] the m.e.p.c. exhibits a rapidly decaying initial component which is not present in Fig. 7*A*. This rapid component occurs during the time of high [ACh] and tends to follow the loss of cleft ACh under these conditions. As the cleft [ACh] falls to negligible values the decay rate slows to r_2, the rate determined by channel kinetics. These values of cleft [ACh] decay times compare well with Magleby & Stevens (1972) driving function decay time of about 300 μsec estimated for twitch fibre evoked end-plate currents in frog. The results illustrate significant changes in

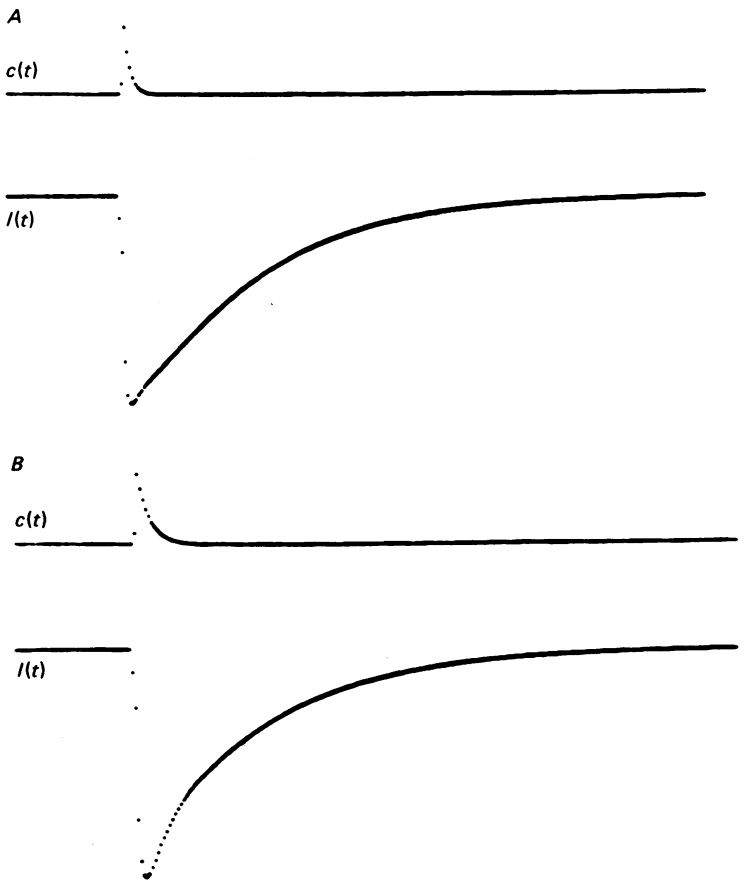

Fig. 7. M.e.p.c. time course predicted by the KM model. These time courses are theoretical descriptions from the KM kinetic scheme in which the [ACh] (plotted as the top trace in each panel) had a peak value of $10K_D$. These large concentrations augment the observed rates which were estimated at zero [ACh]. Because the large concentration is present only briefly the dominant effect is to shorten the m.e.p.c. rise time (compare *A* with Fig. 5*A*). If the [ACh] outlasts the m.e.p.c. time-to-peak, a temporarily increased decay rate can also be observed as in *B*. This effect on the decay rate manifests itself as an event which decays non-exponentially, having a brief rapid decay from its peak. At larger times after the concentration transient has died away the event decays exponentially. These simulations used the same transition rates as those in Fig. 5 and $[ACh]_{peak} = 10K_D$. In *A* the [ACh] decayed with a time constant of approximately 250 μsec; in *B* it was 500 μsec. Time base: 100 μsec per point.

the m.e.p.c. itself which depend upon the time course and cleft concentration of ACh. Although it cannot be demonstrated that these kinds of cleft [ACh] transients occur *in vivo*, they are certainly not inconceivable.

If we assume that the KM kinetic model identified here is an accurate description of the molecular states of the ACh-operated channel in slow fibre end-plates, then these two pieces of evidence argue that at the peak of the m.e.p.c. [ACh] may be greater than the K_D for its binding to the receptors. This is not to say that the assumption of low agonist concentration made throughout is violated. First, most of the m.e.p.c. decay time course occurs when [ACh] is zero, after free ACh is removed by hydrolysis, diffusion and binding. Secondly, the validity of the low concentration limit was demonstrated for the fluctuations and voltage-step data. It is only at the peak of the m.e.p.c. where the ACh concentration appears to be large. Under normal conditions this large concentration lasts so briefly that the only detectable result is a shortening of the time-to-peak. If the high concentration condition lasts a few hundred microseconds the m.e.p.c. can appear to decay in a non-exponential manner.

Single channel conductance. The parsimony of the KM kinetic scheme as applied to slow fibre responses permits consideration of whether the 20 % difference observed between the mean single channel conductance values in twitch and slow fibres (Dionne & Parsons, 1981) is real or apparent. The γ estimates reported were based upon the low concentration assumption, $c^n \ll K_D$; as such, they are *apparent* values. The KM model yields a specific relation between the *true* and *apparent* mean single channel conductance values which depends upon α, β, K_D and c:

$$\gamma_{\text{true}} = \frac{c^n\left(\frac{\alpha+\beta}{\alpha}\right)+K_D}{c^n+K_D}\,\gamma_{\text{apparent}}. \tag{19}$$

Although the data indicated that the low concentration limit was indeed applicable, it is instructive to see what effects concentration and voltage can have on the estimated γ values. In Fig. 8 the ratio $\gamma_{\text{true}}/\gamma_{\text{apparent}}$ was plotted as a function of voltage using the mean voltage dependence of the derived rates α and β from Fig. 6*B*. While $c^n = K_D$ seems an unlikely extreme, it is quite plausible that c^n might attain a value of 0·1 K_D. The value γ_{true} would then be from 5 to 7 % greater than the estimate. If c^n were as great as 0·3 K_D, then γ_{true} would be from 10 to 17 % greater than γ_{apparent}. Dionne & Parsons (1981) described γ_{apparent} as independent of voltage, but their data were not accurate enough to resolve differences as small as these. The most important point then is that γ_{true} in slow fibres is quite possibly several percentage points larger than the mean value of 19·5 pS reported. In contrast, any difference between γ_{true} and the estimated value in twitch fibres might be much smaller. The reason is that while twitch fibre current fluctuations were recorded at mean e.p.c.s about 2 times larger than those from slow fibres, the area per twitch fibre end-plate (and hence the number of channels/end-plate) was at least 10 times greater than that of a slow fibre end-plate. If everything else were the same, this would indicate that the relative concentration of ACh was lower during noise studies on twitch fibres. In turn the conductance ratio in twitch fibres would be nearer unity. Thus the 20 % difference between mean apparent single channel conductances in twitch and slow fibres may not represent a difference between the *true* values. The

slow fibre value may be larger than reported, but the twitch fibre value is probably accurately estimated.

This kinetic description of the data encourages speculation about the molecular mechanism by which a voltage-dependent unbinding rate might arise. One idea is that proposed by Ann Woodhull (1973) to account for H^+ block of the Na channel. If the ACh binding site were embedded in the membrane so that the charged substrate must pass through a portion of the membrane electric field before binding, then

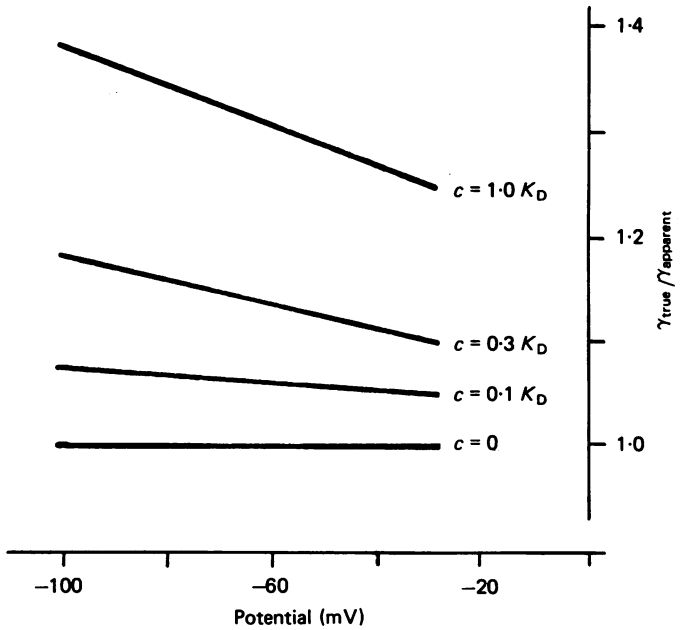

Fig. 8. Agonist concentration and membrane voltage can alter the single channel conductance. Plotted here are the predictions of the KM scheme for the ratio $\gamma_{true}/\gamma_{apparent}$ using eqn. (19). The regression lines fitted in Fig. 6*B* were used to estimate α and β. Relative concentration values of 0, 0·1, 0·3 and 1·0 times K_D were selected to span the range of experimental conditions. Although c was never determined experimentally, it is most probable that $c^n < 0{\cdot}3\ K_D$. Thus, $\gamma_{apparent}$ would underestimate γ_{true} by several percent, and a small voltage dependence of $\gamma_{apparent}$ would go undetected in the experimental scatter.

the field would affect the apparent binding rate. By assuming an ideal membrane in which voltage drops linearly with distance, an estimate of the fractional depth into the membrane for the binding site may be made. For the ACh channel with the $k_2(V)$ given in Fig. 6, the receptor site would appear to reside about a quarter of the way through the membrane. Although this estimate depends critically on the assumed microscopic environment of the binding site, as well as the precise nature of the transition described by rate k_2, it suggests that the concept of an embedded binding site is quite plausible.

The descriptive accuracy of the KM model for both twitch and slow fibre ACh-operated channels is elegant in its simplicity. The essential difference between channels from the two fibre types appears in the lifetimes of the intermediate closed

states which have bound agonist. For twitch fibre responses the assumption of rapid binding and unbinding rates relative to the conformation change rates means that this intermediate state has a negligible lifetime. Functionally then, the fate of a twitch channel in the intermediate state is almost always to unbind the agonist, not open. In contrast the slow fibre channel has an intermediate state lifetime which is appreciable, varying between 1·0 and 1·8 msec with voltage (Fig. 6). Slow fibre cholinergic channels could flutter between open and closed states once agonist molecules have bound. Examples of fluttering in normal single channel records have been reported by Patlak, Sakmann & Neher (1979) and by Nelson & Sachs (1979) and also by Neher & Steinbach (1978) following local anaesthetic treatment. It is this fluttering which appears to produce the added high-frequency spectral noise, the two-component voltage-step response, and the lengthened m.e.p.c. decay time course. The voltage dependence of the intermediate state lifetime is a direct reflection of the voltage-dependent unbinding rate k_2, since the opening rate β appeared not to depend on voltage. This voltage-dependent unbinding is also reflected in the probability (β/k_2) that the channel will open once it is in the intermediate state. As the membrane depolarizes the probability of channel opening decreases because the unbinding rate k_2 increases with the voltage causing β/k_2 to decrease. Such a change is consistent with the apparent physiological role of the slow fibre channels. These channels are the mechanism by which the membrane is depolarized to produce tension; there is no conducted action potential. Thus, when the membrane depolarizes the probability of channels opening decreases. This could aid in both maintenance of the depolarized state and repolarization of the membrane.

A similar mechanism to that described here for the activation of the slow fibre ACh-operated receptor/channel complex may operate when synthetic agonists are used on twitch fibres. Commonly such agonists produce current fluctuations spectra which cannot be fitted by a single Lorentzian line (Colquhoun *et al.* 1975) and the false transmitter acetylmonoethylcholine yields long time course m.e.p.c.s with disparate rates in addition (Colquhoun *et al.* 1977). The simplest idea of how a synthetic agonist might differ from ACh would be that it bound to the receptor with a different equilibrium constant. If this reflected an increased affinity between agonist and receptor, it could allow a longer intermediate state lifetime (scheme 13) and so produce the observed responses.

In this paper I have described how several synaptic responses must be used together in a carefully synchronized manner to test and select for an accurate model from among a number of viable kinetic schemes known formally to describe the data. An interesting point is made, especially by the KM model: a single exponential decay in a response does not necessarily demand that there exist a single rate-limiting step as its determinant. The slow fibre m.e.p.c. decays exponentially although neither binding nor conformational rates alone control the decay time course. Instead, these two processes appear to work together to produce a decay time constant which is greater than either the open channel lifetime or the bound state lifetime. A similar claim could be made for the twitch fibre m.e.p.c. also, but to what extent binding and conformational rates each contribute to the measured decay process there remains unclear.

I wish to thank Dr Charles F. Stevens for his encouragement and advice. It was his suggestion that the voltage-step experiments might test for an extrasynaptic population of ACh-operated channels. This work was supported by U.S. Public Health Service grants (NS 15344 and NS 13581) from the National Institutes of Health.

REFERENCES

ADAMS, P. R. (1974). Kinetics of agonist conductance changes during hyperpolarization at frog end-plates. *Br. J. Pharmac.* **53**, 308–310.

ADAMS, P. R. (1976). Voltage dependence of agonist responses at voltage-clamped frog end-plates. *Pflügers Arch.* **361**, 145–151.

ADAMS, P. R. & SAKMANN, B. (1978*a*). Decamethonium both opens and blocks end-plate channels. *Proc. natn. Acad. Sci. U.S.A.* **75**, 2994–2998.

ADAMS, P. R. & SAKMANN, B. (1978*b*). Agonist-triggered end-plate channel opening. *Biophys. J.* **21**, 53*a*.

ANDERSON, C. R., CULL-CANDY, S. G. & MILEDI, R. (1978). Glutamate current noise: post-synaptic channel kinetics investigated under voltage clamp. *J. Physiol.* **282**, 291–242.

ANDERSON, C. R. & STEVENS, C. F. (1973). Voltage clamp analysis of acetylcholine produced end-plate current fluctuations at frog neuromuscular junction. *J. Physiol.* **235**, 655–691.

BARKER, J. L. & MCBURNEY, R. N. (1979). GABA and glycine may share the same conductance channel on cultured mammalian neurones. *Nature, Lond.* **277**, 234–236.

COLQUHOUN, D. (1973). The relation between classical and co-operative models for drug action. In *Drug Receptors*, ed. RANG, H. P., pp. 149–182. London: Maximillan.

COLQUHOUN, D., DIONNE, V. E., STEINBACH, J. H. & STEVENS, C. F. (1975). Conductance of channels opened by acetylcholine-like drugs in muscle end-plate. *Nature, Lond.* **253**, 204–206.

COLQUHOUN, D. & HAWKES, A. G. (1977). Relaxation and fluctuations of membrane currents that flow through drug-operated channels. *Proc. R. Soc.* B. **199**, 231–262.

COLQUHOUN, D., LARGE, W. A. & RANG, H. P. (1977). An analysis of the action of a false transmitter at the neuromuscular junction. *J. Physiol.* **266**, 361–395.

CULL-CANDY, S. G., MILEDI, R. & TRAUTMANN, A. (1979). End-plate currents and acetylcholine noise at normal and myasthenic human end-plates. *J. Physiol.* **287**, 247–265.

DEL CASTILLO, J. & KATZ, B. (1957). Interaction at end-plate receptors between different choline derivatives. *Proc. R. Soc.* B **146**, 369–381.

DIONNE, V. E. (1979). Modulation of conductance at the neuromuscular junction. *Membrane Transport Processes*, vol. 3, ed. STEVENS, C. F. and TSIEN, R. W., pp. 123–132. N.Y.: Raven.

DIONNE, V. E. & PARSONS, R. L. (1978). Synaptic channel gating differences at snake twitch and slow neuromuscular junctions. *Nature, Lond.* **274**, 902–904.

DIONNE, V. E. & PARSONS, R. L. (1981). Characteristics of the acetylcholine channel in twitch and slow fibre neuromuscular junctions of the garter snake. *J. Physiol.* **310**, 145–158.

DIONNE, V. E., STEINBACH, J. H. & STEVENS, C. F. (1978). An analysis of the dose-response relationship at voltage-clamped frog neuromuscular junctions. *J. Physiol.* **281**, 421–444.

DIONNE, V. E. & STEVENS, C. F. (1975). Voltage dependence of agonist effectiveness at the frog neuromuscular junction: resolution of a paradox. *J. Physiol.* **251**, 245–270.

DUDEL, J. (1978). Relaxation after voltage step of inhibitory synaptic current elicited by nerve stimulation (crayfish neuromuscular junction). *Pflügers Arch.* **376**, 151–157.

GAGE, P. W. & HAMILL, O. P. (1980). Lifetime and conductance of acetylcholine-activated channels in normal and denervated toad sartorius muscle. *J. Physiol.* **298**, 525–538.

GAGE, P. W. & MCBURNEY, R. N. (1975). Effects of membrane potential, temperature and neostigmine on the conductance change caused by a quantum of acetylcholine at the toad neuromuscular junction. *J. Physiol.* **244**, 385–407.

KARLIN, A. (1967). On the application of a plausible model of allosteric proteins to the receptor for acetylcholine. *J. theor. Biol.* **16**, 306–320.

KATZ, B. & MILEDI, R. (1970). Membrane noise produced by acetylcholine. *Nature, Lond.* **226**, 962–963.

KUFFLER, S. W. & YOSHIKAMI, D. (1975). The number of transmitter molecules in a quantum: an estimate from iontophoretic application of acetylcholine at the neuromuscular synapse. *J. Physiol.* **251**, 465–482.

MAGLEBY, K. L. & STEVENS, C. F. (1972). A quantitative description of end-plate currents. *J. Physiol.* **223**, 173–199.

MATTHEWS-BELLINGER, J. & SALPETER, M. M. (1978). Distribution of acetylcholine receptors at frog neuromuscular junctions with a discussion of some physiological implications. *J. Physiol.* **279**, 197–213.

NEHER, E. & STEVENS, C. F. (1977). Conductance fluctuations and ionic pores in membranes. *A. Rev. Biophys. Bioeng.* **6**, 345–381.

NEHER, E. & SAKMANN, B. (1975). Voltage-dependence of drug-induced conductance in frog neuromuscular junction. *Proc. natn. Acad. Sci. U.S.A.* **72**, 2140–2144.

NEHER, E. & SAKMANN, B. (1976). Noise analysis of drug induced voltage clamp currents in denervated frog muscle fibres. *J. Physiol.* **285**, 705–729.

NEHER, E. & STEINBACH, J. H. (1978). Local anesthetics transiently block currents through single acetylcholine-receptor channels. *J. Physiol.* **277**, 153–176.

NELSON, D. J. & SACHS, F. (1979). Single ionic channels observed in tissue-cultured muscle. *Nature, Lond.* **282**, 861–863.

PATLACK, J., SAKMANN, B. & NEHER, E. (1979). Gating kinetics of single acetylcholine activated channels measured during 'bursts' of activity following desensitization. *Biophys. J.* **25**, 67*a*.

SHERIDAN, R. E. & LESTER, H. A. (1977). Rates and equilibria of the acetylcholine receptor of *Electrophorus* electroplaques. *J. gen. Physiol.* **70**, 187–219.

THRON, C. D. (1973). On the analysis of pharmacological experiments in terms of an allosteric receptor model. *Molec. Pharmacol.* **9**, 1–9.

WOODHULL, A. M. (1973). Ionic blockage of sodium channels in nerve. *J. gen. Physiol.* **61**, 687–708.